

Validation of a Model for the Complex of HIV-1 Reverse Transcriptase with Sustiva through Computation of Resistance Profiles

Robert C. Rizzo, De-Ping Wang, Julian Tirado-Rives, and William L. Jorgensen*

Department of Chemistry, Yale University
New Haven, Connecticut 06520-8107

Received August 21, 2000

Revised Manuscript Received October 24, 2000

All retroviruses depend on a virally encoded reverse transcriptase enzyme (RT) to convert viral RNA into DNA for subsequent incorporation into the host cell genome.¹ Drug-design efforts to arrest reverse transcription in HIV have led to the FDA approval of three non-nucleoside reverse transcriptase inhibitors (NNRTIs), nevirapine, delaviridine, and efavirenz (Sustiva). Additional compounds, including MKC-442, are in clinical trials (Table 1). Because of the low fidelity of HIVRT, the mutation rate in the encoded proteins including HIVRT is great.^{2,3} As a result, all HIVRT inhibitors incur resistance problems that adversely affect their clinical value.^{4,5} A measure of a drug's effectiveness against a mutation is given by the fold resistance, which is the ratio of mutant to wild-type activities. Sustiva has been shown to remain notably active against several common HIVRT point mutations including Val → Ala at position 106 (V106A) and Tyr → Cys at position 181 (Y181C) (Table 1).

No HIVRT structure with Sustiva has been reported that may help explain its improved resistance profile. Herein, we have (a) computed a structure for the Sustiva/HIVRT complex, (b) validated the structure through computations of the effects of the V106A and Y181C mutations on binding affinities for four drugs, and (c) obtained structural insights on the improved effectiveness of Sustiva. A binding site model⁶ was constructed from the 2.55-Å crystal structure of the MKC-442/HIVRT complex (pdb 1rt1)⁷ with MKC-442 removed including only those residues within ~15 Å of MKC-442. The MATADOR program⁸ was then used to dock Sustiva into the NNRTI site.⁹ The other complexes were prepared analogously starting with coordinates from the X-ray structures of nevirapine (pdb 1vrt),¹⁰ HEPT (pdb 1rti),⁷ and 9-Cl TIBO (pdb 1rev)¹¹ bound to HIVRT. The docking calculations placed Sustiva in a reasonable position and orientation in the binding site in comparison with the crystal structures for the complexes with MKC-442, nevirapine, and 9-Cl TIBO (Figure 1). As controls, MKC-442, nevirapine, 9-Cl TIBO, and HEPT were also docked back into their binding sites to verify that the docking protocol could reproduce experimental structures. The lowest-energy structure generated during the docking runs was taken as the "best" structure and was found in all cases to reproduce closely the position and orientation observed in the crystal structures; the rmsd for the non-hydrogen atoms of the four ligands between

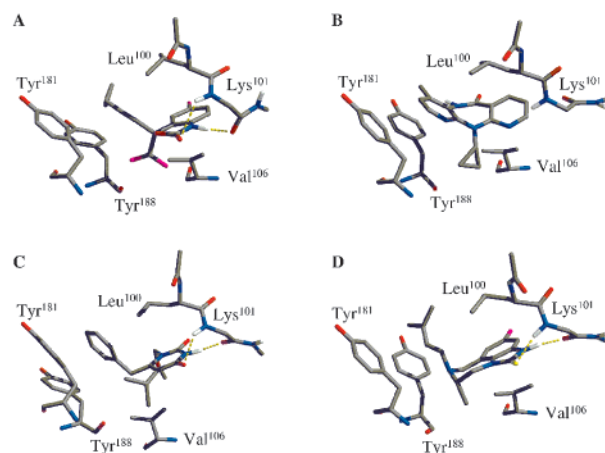


Figure 1. Orientation of the four NNRTIs in the HIVRT binding site. (A) Best docked structure of Sustiva. (B) Nevirapine from pdb entry 1vrt. (C) MKC-442 from pdb entry 1rt1. (D) 9-Cl TIBO from pdb entry 1rev.

the X-ray and docked structures was 0.43–0.60 Å. These low rmsd values and the limited flexibility of Sustiva are favorable for the accuracy of the docking calculations.

The best docked structure of Sustiva reveals that it makes interactions that are consistent with those for other NNRTIs and that it overlays well with the "butterfly" shape of nevirapine. Unlike nevirapine, hydrogen bonds are present between Sustiva and the protein backbone at position Lys101 that are similar to those observed in the crystal structures with 9-Cl TIBO and MKC-442 (Figure 1). Nevirapine makes no formal ligand–protein hydrogen bonds, but it does form a π -type hydrogen bond between the secondary amide hydrogen and Tyr188¹² and water-mediated hydrogen bonds.^{10,12} The cyclopropyl ethynyl group of Sustiva is positioned toward aromatic residues Tyr181 and Tyr188 in the same fashion as the methylpyridine fragment of nevirapine, the benzyl ring of MKC-442, and the dimethylallyl group of 9-Cl TIBO (Figure 1). Presumably, these aryl- π interactions all contribute favorably to binding.^{4,5} Superposition based on the HIVRT C α atoms shows that these π fragments of the inhibitors coincide spatially in the binding site and that Sustiva's π fragment is the smallest (Figure 2).

An alternative binding mode suggested by Maga et al. was based on an alignment of nevirapine and Sustiva in which the

(9) MATADOR uses a Monte Carlo-based Tabu search algorithm. To keep the Tabu search focused on the known NNRTI binding site during the docking runs, a 50 kcal/mol Å² half-harmonic restraining force was applied if the distance between the ligand and the binding site center was greater than 5 Å. The defined binding site was roughly centered on the alkyne group of Sustiva. The Tabu list was set to be 25 and constructed from unique structures considering energetic as well as geometric criteria. In total, 100 Tabu cycles were performed with each Tabu search generating 100 randomly placed ligand positions around the binding site. The decision to accept a new structure onto the Tabu lists is made after an intermolecular energy minimization and is based on both energetic and geometric criteria. The protein and ligand were rigid during the docking. The CM1P augmented OPLS-AA force field [Duffy, E. M.; Jorgensen, W. L. *J. Am. Chem. Soc.* 2000, 122, 2878–2888] provided the initial structure of Sustiva; it was also used to determine the nonbonded energies, which were stored on a spherical grid for efficiency. The total intermolecular interactions between the ligand and protein amount to a measure of both steric and electrostatic complementarity; the lowest energy structure found during the simulations was taken as the "best" docked system. A distance-dependent dielectric constant of 4 ($\epsilon = 4r$) was used for all docking calculations.

(10) Ren, J.; Esnouf, R.; Garman, E.; Somers, D.; Ross, C.; Kirby, I.; Keeling, J.; Darby, G.; Jones, Y.; Stuart, D.; et al. *Nat. Struct. Biol.* 1995, 2, 293–302.

(11) Ren, J.; Esnouf, R.; Hopkins, A.; Ross, C.; Jones, Y.; Stammers, D.; Stuart, D. *Structure* 1995, 3, 915–26.

(12) Rizzo, R. C.; Tirado-Rives, J.; Jorgensen, W. L. *J. Med. Chem.* 2000, 0000, 0000–0000. In press.

(1) Katz, R. A.; Skalka, A. M. *Annu. Rev. Biochem.* 1994, 63, 133–173.

(2) Preston, B. D.; Poiesz, B. J.; Loeb, L. A. *Science* 1988, 242, 1168–1171.

(3) Roberts, J. D.; Bebenek, K.; Kunkel, T. A. *Science* 1988, 242, 1171–1173.

(4) Tantillo, C.; Ding, J. P.; Jacobomolina, A.; Nanni, R. G.; Boyer, P. L.; Hughes, S. H.; Pauwels, R.; Andries, K.; Janssen, P. A. J.; Arnold, E. *J. Mol. Biol.* 1994, 243, 369–387.

(5) De Clercq, E. *Antiviral Res.* 1998, 38, 153–179.

(6) Protein residues included in the binding site model were 91–110A, 161–205A, 222–242A, 316–321A, 343–349A, 381–383A, and 134–140B.

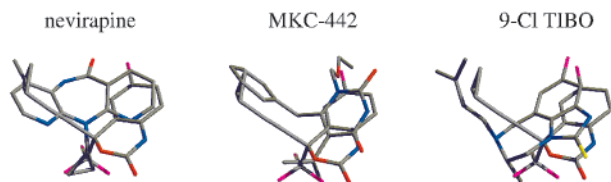
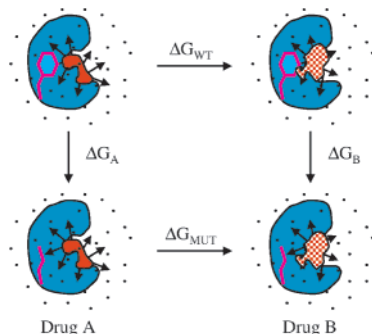
(7) Hopkins, A. L.; Ren, J. S.; Esnouf, R. M.; Willcox, B. E.; Jones, E. Y.; Ross, C.; Miyasaka, T.; Walker, R. T.; Tanaka, H.; Stammers, D. K.; Stuart, D. I. *J. Med. Chem.* 1996, 39, 1589–1600.

(8) Plouffe Price, M. L. Ph.D. Thesis, Yale University, 2000.

Table 1. Relative Free Energies of Binding (ΔG_{FR}) Estimated from Fold Resistance (FR) Values^g

Fold Resistance	Sustiva		Nevirapine			MKC-442		9-Cl TIBO		
	K_i^a	IC_{50}^b	IC_{50}^c	IC_{50}^b	EC_{50}^f	EC_{50}^d	EC_{50}^e	IC_{50}^c	IC_{50}^f	EC_{50}^f
Y181C/WT	0.59	0.11	3.30	2.79	3.49	2.90	5.04	1.64	1.00	2.86
V106A/WT	0.54	0.70	2.81	2.88	3.49	2.92		1.20	1.76	2.02
L100I/WT	1.09	1.91	1.32	0.98	1.57	1.42		2.96		2.80
Y188C/WT		0.81	3.24	2.29				1.99		
K103N/WT	1.11	1.79	1.96	2.26		3.99		2.56		

^a Young, S. D.; Britcher, S. F.; Tran, L. O.; Payne, L. S.; Lumma, W. C.; Lyle, T. A.; Huff, J. R.; Anderson, P. S.; Olsen, D. B.; Carroll, S. S.; Pettibone, D. J.; O'Brien, J. A.; Ball, R. G.; Balani, S. K.; Lin, J. H.; Chen, I. W.; Schleif, W. A.; Sardana, V. V.; Long, W. J.; Byrnes, V. W.; Emini, E. A. *Antimicrob. Agents Chemother.* **1995**, *39*, 2602–2605. ^b Levin, J. http://www.natap.org/reports/NR5-nnr1_update2.resis.htm. ^c Byrnes, V. W.; Sardana, V. V.; Schleif, W. A.; Condra, J. H.; Waterbury, J. A.; Wolfgang, J. A.; Long, W. J.; Schneider, C. L.; Schlabach, A. J.; Wolanski, B. S.; Graham, D. J.; Gotlib, L.; Rhodes, A.; Titus, D. L.; Roth, E.; Blahy, O. M.; Quintero, J. C.; Staszewski, S.; Emini, E. A. *Antimicrob. Agents Chemother.* **1993**, *37*, 1576–1579. ^d Balzarini, J.; Baba, M.; Declercq, E. *Antimicrob. Agents Chemother.* **1995**, *39*, 998–1002. ^e Baba, M.; Shiget, S.; Yuasa, S.; Takashima, H.; Sekiya, K.; Ubasawa, M.; Tanaka, H.; Miyasaka, T.; Walker, R. T.; Declercq, E. *Antimicrob. Agents Chemother.* **1994**, *38*, 688–692. ^f Balzarini, J.; Karlsson, A.; Meichsner, C.; Paessens, A.; Riess, G.; Declercq, E.; Kleim, J. P. *J. Virol.* **1994**, *68*, 7986–7992. ^g FR = mutant/wild-type activities, $\Delta G_{FR} = RT \ln FR$ in kcal/mol. The columns show the structure, compound name, the assay type and reference for the FR values, and ΔG_{FR} for several common HIVRT mutations.

**Figure 2.** Overlays of the binding-site positions of nevirapine, MKC-442, and 9-Cl TIBO with Sustiva in CPK colors.**Figure 3.** Thermodynamic cycle used to compute *relative* fold resistance values. The wild-type side-chain (magenta) is perturbed to the mutant side chain in the presence of Drug A (solid red) and Drug B (checked red) while bound to a protein (cyan). Relative fold resistance = $\Delta G_B - \Delta G_A = \Delta G_{MUT} - \Delta G_{WT}$.

amide moiety of both drugs was superimposed.¹³ The present docking calculations did not find this orientation. Furthermore, forced placement of Sustiva in this alternative geometry yielded steric and electrostatic protein–ligand interaction energies ~ 5 and 15 kcal/mol, respectively, less favorable than for our docked structure. The alternative orientation is unlikely since the hydrogen bonds to the backbone of Lys101 would be sacrificed.

A computational experiment was then pursued to validate the Sustiva model by predicting relative fold resistance values. The methodology, which is a general computational approach to determining the impact of protein mutations on drug candidates, hinges on the thermodynamic cycle in Figure 3. For two inhibitors, A and B, ΔG_{WT} and ΔG_{MUT} are the differences in free energy of binding for B vs A with the wild-type and mutant proteins,

(13) Maga, G.; Ubiali, D.; Salvetti, R.; Pregnotato, M.; Spadari, S. *Antimicrob. Agents Chemother.* **2000**, *44*, 1186–1194.

respectively, while ΔG_A and ΔG_B are the changes in free energy of binding for A and B with the mutant vs the wild-type protein. The quantities are related as $\Delta G_{MUT} - \Delta G_{WT} = \Delta G_B - \Delta G_A = \Delta \Delta G$, where $\Delta \Delta G$ is the experimentally observable difference in the fold resistance values, $RT \ln FR_B - RT \ln FR_A$. The FR activity ratios from IC or EC values are expected to parallel binding constant ratios for similar inhibitors.¹⁴ Computationally, one could mutate either the drug or the protein. However, we have chosen to perform the structurally simpler mutations of the protein; specifically, Val106 was mutated to Ala, and Tyr181 was mutated to Cys in the presence of the four NNRTIs. Our results should yield the observed experimental trends, if the proposed Sustiva/HIVRT structure is correct.

Molecular dynamics (MD)¹⁵ equilibration and Monte Carlo¹⁶ free energy perturbation (MC/FEP)¹⁷ simulations were performed on the docked Sustiva structure and the equivalent nevirapine, MKC-442, and 9-Cl TIBO binding-site models, including 850 water molecules in the FEP calculations. Aside from normal thermal oscillations, the positioning of Sustiva in the binding site from the docking calculations was maintained in the MD and MC simulations. There is significant variability in the reported fold resistance data, presumably due to the use of different assay conditions (Table 1). Sustiva, however, consistently emerges as more tolerant toward the Y181C and V106A mutations than the

(14) Cheng, Y.; Prusoff, W. H. *Biochem. Pharmacol.* **1973**, *22*, 3099–3108.

(15) The docked Sustiva/HIVRT structure was subjected to a molecular dynamics (MD) simulation to allow the HIVRT backbone and side chains to relax. The CM1P augmented OPLS-AA force field was used for all MD simulations with the IMPACT program [Levy, R. M. et al., *IMPACT Version 1.00*; Schrödinger, Inc.: Jersey City, NJ, 1999]. Ten cycles of gradient-based energy minimization were performed prior to the MD simulations, and the complex was then restrained in the following manner. Protein residues were allowed to move freely within ~ 10 Å of the binding site (95–107A, 172A, 177–182A, 188–192A, 198A, 227A, 229A, 234–236A, 318–319A, 321A, and 135–139B). Movement was restrained for those residues in a 10–12 Å shell about the binding site, i.e., for residues 94A, 108A, 175–176A, 183A, 187A, 225A, 237–239A, 317A, 320A, 349A, 382–383A, 134B, 140B with harmonic potentials. All other residues were restrained to their positions after conjugate-gradient minimization. The Verlet algorithm was used to integrate Newton's equations of motion using a time step of 0.001 ps and constant temperature was maintained through coupling to a Berendsen temperature bath using a relaxation parameter of 0.2 ps for the velocity scaling. Bond lengths were fixed by the SHAKE algorithm and a distance-dependent dielectric constant of 4 ($\epsilon = 4r$) was used. First, 3 ps of initial equilibration was performed at 100 K followed by 50 ps of equilibration at 300 K. Quenching of the structure was performed by reducing the simulation temperature over 6 blocks of 4 ps each starting at 300 K and ending at 50 K. The same MD equilibration was also performed on the nevirapine, MKC-442, and the 9-Cl TIBO structures, and the resultant complexes were then used in the MC simulations.

Table 2. Relative Fold Resistance Energies ($\Delta\Delta G$) in kcal/mol for HIV-1 RT Mutations normalized to Sustiva

inhibitor	$\Delta\Delta G$ for Y181C		$\Delta\Delta G$ for V106A	
	calcd	exptl ^a	calcd	exptl ^a
Sustiva	0.00	0.00	0.00	0.00
nevirapine	3.88 \pm 0.3	2.20, 2.71, 2.90	3.33 \pm 0.4	2.34, 2.27, 2.95
MKC-442	4.70 \pm 0.3	2.31, 4.45	0.72 \pm 0.5	2.38
9-Cl TIBO	3.01 \pm 0.3	1.05, 0.41, 2.27	1.32 \pm 0.5	0.66, 1.22, 1.48

^a Values derived from Table 1.

other drugs, especially nevirapine and MKC-442. Indeed, the present FEP results do predict Sustiva to be less affected by both mutations than the other three inhibitors (Table 2). The agreement of the computed free energies with the experimental results strongly supports the correctness of our docked model.

The structural model suggests some factors that render Sustiva less affected by the Y181C and V106A mutations in comparison with the other compounds. It is well-known that the NNRTI binding site is capable of accommodating structurally diverse inhibitors and that different inhibitors give rise to strikingly different patterns of resistance mutations among ~ 15 residues that line the binding site.^{4,5} In general, this variability implies that the effect of mutations on drug binding needs assessment on a case-by-case basis. However, the Y181C mutant arises early and confers resistance for many NNRTIs. This can be attributed to the loss of favorable aryl/ π interactions, for example, between the tyrosine and the methylpyridyl and benzyl rings of nevirapine and MKC-442, and the dimethylallyl group of 9-Cl TIBO (Figure 1). Loss of the interaction between Tyr181 and the smaller, less polarizable cyclopropyl ethynyl group of Sustiva is expected to be less detrimental.

In the case of V106A, the residue is tucked under the benzene ring of Sustiva and is in van der Waals' contact with the trifluoromethyl group. Reduction of these interactions appears to

(16) Each protein-inhibitor complex was briefly energy-minimized prior to the Monte MC simulations using a distance-dependent dielectric constant of 4 ($\epsilon = 4r$). The CMIP augmented OPLS-AA force field was used with the MCPRO program [Jorgensen, W. L. *MCPRO Version 1.65*; Yale University; New Haven, CT, 2000]. For the MC simulations, a water cap with a 22-Å radius was used containing ~ 850 TIP4P water molecules and the system was partitioned into rigid residues (91–94A, 109–110A, 116–178A, 184–185A, 192–197A, 199–205A, 222–224A, 230–232A, 240–242A, 316–317A, 320–321A, 343–349A, 381–383A, 134–135B, 137B, 140B) and flexible residues (95–108A, 179–183A, 186–191A, 198A, 225–229A, 233–239A, 318–319A, 136B, 138B). All HIVRT side chains within ~ 10 Å from the center of the water cap were sampled, the protein backbone was fixed, and each inhibitor was fully flexible. Each solvated complex was subjected to 1 million configurations of solvent-only equilibration, 10 million of equilibration, and 10 million configurations of averaging per window during the FEP simulations. For additional MC simulation parameters and protocols, see ref 12.

(17) For a recent discussion of FEP methodology, see: Jorgensen, W. L. Free Energy Changes in Solution. In *Encyclopedia of Computational Chemistry*; Schleyer, P. v. R., Ed.; Wiley: New York, 1998; Vol. 2, pp 1061–1070.

be partly compensated by better alignment of the NH–O hydrogen bond with Lys101 when the buttressing effect of the valine side chain is reduced by conversion to alanine. In the MC simulations, the hydrogen bond between the oxazinone NH of Sustiva and the carbonyl oxygen of Lys101 is on average 0.1 Å shorter (1.77 vs 1.85 Å) when residue 106 is Ala rather than Val. The interaction of the valine's isopropyl group with the weakly polarizable trifluoromethyl group is also likely less attractive than the corresponding interactions with the cyclopropyl group of nevirapine and the isopropyl and ethoxymethyl groups of MKC-442 (Figure 1). Thus, it is reasonable to propose, on the basis of the present structure, that Sustiva's improved resistance profile benefits from a combination of less favorable initial interactions with Tyr181 and Val106 and more favorable hydrogen bonding with Lys101 in the V106A mutant. Consistently, the L100I mutation is more damaging (Table 1) because Leu100 forms a snug lid over the ring systems for all four inhibitors (Figure 1). Without adjustment, the branching at C β rather than C γ would direct the methyl group of Ile100 directly into the rings. An alternative strategy for improved resistance profiles is to enhance interactions with immutable residues such as Trp229.¹⁸

In this work, we have presented a molecular model for the important anti-HIV drug Sustiva bound to HIVRT. The resultant structure reveals that Sustiva overlays well with the butterfly shape of nevirapine and makes similar contacts with HIVRT as do other reported NNRTIs including hydrogen bonds with the backbone of Lys101 (Figure 1). FEP methodology for the assessment of relative resistance profiles for drug candidates has been defined. Results from its application to four NNRTIs (Table 2) are in good agreement with the experimental activity trends and provide evidence that the proposed binding mode for Sustiva is correct. Sustiva's relative insensitivity to the Y181C and V106A mutants appears to arise from a mix of relatively weaker interactions with Tyr181 and Val106 and improvement of hydrogen bonding for Ala106. These findings highlight the power of molecular modeling for structure and binding affinity predictions and its potential for structure-based drug design.

Acknowledgment. This work was supported by the National Institute of Allergy and Infectious Diseases (AI44616). We thank Melissa L. Plouffe for computational assistance with the docking calculations, and Dr. Marilyn B. Kroeger Smith, Professor Richard H. Smith, and Mark A. Wilson for helpful discussions.

Note Added in Proof. A crystal structure has now appeared for a Sustiva/HIVRT complex [Ren, J.; Milton, J.; Weaver, K. L.; Short, S. A.; Stuart, D. I.; Stammers, D. K. *Structure* **2000**, *8*, 1089–1094]. It fully confirms the correctness of the structure predicted here.

JA003113R

(18) Hopkins, A. L.; Ren, J.; Tanaka, H.; Baba, M.; Okamoto, M.; Stuart, D. I.; Stammers, D. K. *J. Med. Chem.* **1999**, *42*, 4500–4505.